Use of an Imperfect Neutral Diluent and Outer Vesicle Layer Scooting Mode Hydrolysis To Analyze the Interfacial Kinetics, Inhibition, and Substrate Preferences of Bee Venom Phospholipase A_2[†]

Bao-Zhu Yu,[‡] Farideh Ghomashchi,[§] Yolanda Cajal,[‡] Robert R. Annand,[§] Otto G. Berg,*[,∥] Michael H. Gelb,*[,§] and Mahendra K. Jain*[,‡]

Department of Chemistry and Biochemistry, University of Delaware, Newark, Delaware 19716, Departments of Chemistry and Biochemistry, University of Washington, Seattle, Washington 98195-1700, and Department of Molecular Biology, Uppsala University Biomedical Center, Uppsala, Sweden

Received June 25, 1996; Revised Manuscript Received January 6, 1997[⊗]

ABSTRACT: Interfacial catalytic constants for bee venom phospholipase A_2 (bvPLA2) have been obtained for its action on vesicles of the anionic phospholipid 1,2-dimyristoylphosphatidylmethanol (DMPM) in the highly processive scooting mode. Spectroscopic measurements which directly measure transbilayer movement of membrane components show that this exchange does not occur in anionic vesicles that have undergone complete bvPLA2-catalyzed hydrolysis of all phospholipids in the outer vesicle monolayer. 3-Hexadecyl-*sn*-glycero-1-phosphocholine (D-LPC) is an adequate neutral diluent for bvPLA2, which is defined as an amphiphile that forms an aggregate to which enzyme binds but neutral diluent molecules bind weakly in the enzyme's active site. D-LPC has weak affinity for the active site of bvPLA2, and theory and protocols are developed that allow its use to determine equilibrium dissociation constants for competing active site ligands. Some of the properties of bvPLA2 are shared by other 14 kDa PLA2s. (1) Ca^{2+} is required for binding of ligands to the active site but not for the binding of enzyme to the interface. (2) bvPLA2 does not significantly discriminate between phospholipids with different polar head groups or acyl chains. (3) bvPLA2 does not bind to phosphatidylcholine vesicles, and binding occurs if anionic amphiphiles are present in the vesicle. Novel features of bvPLA2 include the following: (1) Neutral diluents for other 14 kDa phospholipases A_2 are not neutral diluents for bvPLA2. (2) Saturation of the active site with a variety of different ligands does not completely prevent histidine alkylation by 2-bromo-4′-nitroacetophenone, and Ca^{2+} binding does not change the rate of histidine alkylation. Finally, the carbohydrate portion of bvPLA2 does not alter the interfacial catalytic properties of the enzyme. Kinetic analysis of bvPLA2 in the scooting mode together with previous studies with other 14 kDa PLA2s provides a paradigm for the quantitative analysis of interfacial catalysis.

Bee venom phospholipase A_2 (bvPLA2)[1] is a member of a class of small (∼14−16 kDa) secreted enzymes that cleave the *sn*-2 ester of glycerophospholipids (Dennis, 1983; Gelb et al., 1995; Verheij et al., 1981; Waite, 1987). The amino acid sequences of secreted PLA2s can be organized into type I (found in tissues, including pancreas and spleen, and venoms of elapid snakes of the Old World) and type II (found in inflammatory cells, including platelets and mast cells, and venoms of crotalids and viperids of the New World) subtypes on the basis of the location of disulfides and the presence of small insertions and deletions (Davidson & Dennis, 1990; Heinrikson et al., 1977; van den Bergh et al., 1989). The primary structure of bvPLA2 (Kuchler et al., 1989) as well as the enzymes from Gila monster and lizard venoms (Gomez et al., 1989; Sosa et al., 1986) form a distinct group (type III) that display homology to type I and II enzymes only in the Ca^{2+} binding loop and in short peptide sections that contribute catalytic residues. X-ray crystallographic analysis of bvPLA2 shows that its global structure is very different than those of type I and II enzymes, but the active site and Ca^{2+} binding residues are nearly superimposable for enzymes of all three types (Scott & Sigler, 1994). All three types of enzymes have interfacial recognition regions that include a

[†] This work was supported by Grants GM29703 to M.K.J. and HL36235 to M.H.G., Research Career Development Award GM562 to M.H.G., and Postdoctoral Fellowship GM15464 to R.R.A., all from the National Institutes of Health.

* To whom correspondence should be addressed.
[‡] University of Delaware.
[§] University of Washington.
[∥] Uppsala University Biomedical Center.

[⊗] Abstract published in *Advance ACS Abstracts,* March 15, 1997.

[1] Abbreviations: BAPTA, 1,2-bis(2-aminophenoxy)ethane-*N*,*N*,*N*′,*N*′-tetraacetic acid; bis-PC, two molecules of 1-palmitoyl-*sn*-glycero-3-phosphocholine esterified via their *sn*-2 hydroxyl groups to HOOC-$(CH_2)_{30}$-COOH; bvPLA2, 16 kDa phospholipase A_2 from the venom of honey bees (*Apis mellifera*); dansyl-DTPE, *N*-dansyl-1,2-ditetradecyl-*sn*-glycero-3-phosphoethanolamine; D-LPC, 3-hexadecyl-*sn*-glycero-1-phosphocholine; EGTA, ethylene glycol bis(β-aminoethyl ether)-*N*,*N*,*N*′,*N*′-tetraacetic acid; MG14, 1-octyl-2-(phosphonoheptyl)-*sn*-glycero-3-phosphoethanolamine; MJ33, *rac*-1-hexadecyl-3-(trifluoroethyl)-*sn*-glycero-2-phosphomethanol; ND, neutral diluent; PLA2, phospholipase A_2; PNBr, 2-bromo-4′-nitroacetophenone. For phospholipids, the first two letters designate the acyl or alkyl chains at the *sn*-1 and *sn*-2 positions of the glycerol backbone, respectively (A, arachidonyl; M, myristoyl; O, oleoyl; P, palmitoyl; S, stearoyl; and T, tetradecyl), and the last two letters designate the *sn*-3 glycerophosphodiester group (PA, phosphate; PC, phosphocholine; PE, phosphoethanolamine; PM, phosphomethanol; and PS, phosphoserine). If the two fatty acids attached to glycerol are the same, the abbreviation D is used for di; thus, DMPM is 1,2-dimyristoyl-*sn*-glycero-3-phosphomethanol. Radiolabeled phospholipids are designated with the name of the isotope, which is always in the *sn*-2 acyl chain.

S0006-2960(96)01541-3 CCC: $14.00

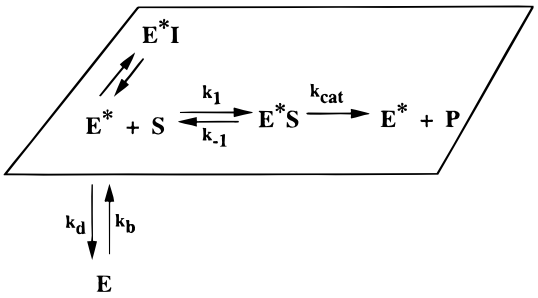

FIGURE 1: Kinetic scheme to describe interfacial catalysis. The enzyme in the aqueous phase (E) must bind to the interface to gain access to its substrate. The enzyme at the interface (E*) can bind a substrate molecule in its active site to give the Michaelis complex E*·S which can go on to products. E* can also bind a competitive inhibitor in the interface to give E*·I. Scooting mode hydrolysis occurs when E* remains at the interface and catalyzes many reaction cycles.

collar of cationic and hydrophobic residues that surround the entrance to the active site slot (Ramirez & Jain, 1991; Scott & Sigler, 1994). Together, these structural features provide a basis for interfacial catalysis, including the tight binding of secreted PLA2s to anionic phospholipid vesicles (Gelb et al., 1995; Jain et al., 1995).

A dissection of interfacial catalysis by PLA2s into the binding of the enzyme to the interface and into the events that occur in the catalytic site (Figure 1) is critical for developing an analytical understanding of the reaction cycle. The analysis of interfacial kinetics has been more difficult than that for enzymes that operate in a homogeneous aqueous environment. It has been shown that interfacial catalysis can be quantitatively and analytically understood in terms of the Michaelis-Menten formalism for the steps of the reaction cycle that occur at the interface (those in the box of Figure 1) (Jain et al., 1986, 1995; Jain & Berg, 1989; Gelb et al., 1995). The kinetic and equilibrium parameters for the interfacial steps shown in Figure 1 can be extracted only if the enzyme is operating in the highly processive scooting mode (Berg et al., 1991; Jain et al., 1986) in which the enzyme, substrate, or products do not leave the interface during the reaction progress. This occurs for secreted PLA2s acting on vesicles of anionic phospholipids. Since the enzyme binds irreversibly to such vesicles, the E to E* step shown in Figure 1 occurs only in the pre-steady-state phase of the reaction, i.e. just after the addition of enzyme to vesicles. In this study, the action of bvPLA2 in the scooting mode was characterized to determine most of the kinetic constants, and the interfacial kinetic properties of bvPLA2 were compared to those of other secreted PLA2s. Key differences between bvPLA2 and other secreted PLA2s are emphasized by the analytical formalism developed in the Appendix.

MATERIALS AND METHODS

Materials. POPC and *N*-(7-nitro-2-1,3-benzoxadiazol-4-yl)dioleoylphosphatidylethanolamine are from Avanti Polar Lipids. Syntheses of the phospholipids DMPM (Jain & Gelb, 1991), DTPC and DTPM (Jain et al., 1986), MJ33 (Jain et al., 1991c), MG14 (Yuan et al., 1990), and dansyl-DTPE (Jain & Vaz, 1987) have been described elsewhere. D-LPC was prepared by methanolysis of 3-hexadecyl-2-myristoyl-*sn*-glycero-1-phosphocholine in the presence of tributylammonium hydroxide. The latter phospholipid was prepared by treating the racemic phospholipid with porcine pancreatic PLA2 in an ether/buffer emulsion (Eibl et al., 1983). The racemic phospholipid was prepared from racemic 1-hexadecyl-*sn*-glycero-3-phosphocholine. Bis-PC was obtained as a generous gift from Prof. Bruce Lennox (McGill University). Native bvPLA2 was obtained from Boehringer, and it was judged to be >90% pure by SDS−PAGE. Recombinant bvPLA2 produced in *Escherichia coli* was obtained as described (Dudler et al., 1992). The mutant of bvPLA2 in which histidine-34 is changed to glutamine has been described (Annand et al., 1996). For all studies with bvPLA2, enzyme solutions were made in borosilicate tubes, since the enzyme sticks to plastic tubes. In this context, bvPLA2 is similar to pancreatic PLA2, but the PLA2 from human synovial fluid binds to glass but not plastic.

Kinetic Studies in the Scooting Mode. Preparation of sonicated DMPM vesicles and protocols for monitoring reaction progress for the hydrolysis of DMPM vesicles in the scooting mode have been described elsewhere for porcine pancreatic PLA2 (Berg et al., 1991; Jain & Gelb, 1991; Jain et al., 1986). Typically, hydrolysis of sonicated DMPM vesicles was monitored by the pH-stat method in a 4 mL reaction mixture containing 0.3 mM DMPM, 1 mM NaCl, and 0.5 mM $CaCl_2$ at pH 8.0 and 22 °C. The reaction progress without intervesicle exchange of substrate was monitored after initiating the reaction with 0.2 μg of bvPLA2, and values of $N_s k_i$ and ν_o (all rate and equilibrium constants are defined in the Results and in the Appendix) were determined. The kinetic parameters were obtained by nonlinear regression fitting of the progress curve to eq 3. To extend the time period for the zero-order phase of the reaction progress, 20 μg of polymyxin B sulfate (Sigma) was added before or after initiating the reaction with 0.02−0.1 μg of bvPLA2, and the Ca^{2+} concentration was 1 mM (Cajal et al., 1995, 1996; Jain et al., 1991b). Other conditions are given in the legend to Figure 3. For inhibition studies, the inhibitor was added before polymyxin B and enzyme except as noted.

Radiometric experiments to show that bvPLA2 binds irreversibly to DMPM vesicles were carried out with the standard assay described above using 0.5 mM $CaCl_2$ and in the absence of polymyxin B sulfate. Five minutes after addition of bvPLA2 to DMPM vesicles, an equal portion of DMPM vesicles containing [^{3}H]DPPC (4000 cpm, 2×10^{-7} mole fraction) was added to the reaction mixture. After an additional 10 min, the reaction was quenched, and tritiated palmitic acid was quantified as described (Ghomashchi et al., 1991a).

Transbilayer movement of phospholipids (flip-flop) was measured using the dithionite method (Hoekstra et al., 1993; McIntyre & Sleight, 1991). An aliquot of sonicated vesicles of DMPM/POPC/*N*-(7-nitro-2-1,3-benzoxadiazol-4-yl)dipalmitoyl phosphatidylethanolamine (64:30:6) (total lipid, 110 μM) was added to 1.5 mL of 10 mM Tris buffer at pH 8.0 saturated with nitrogen with constant stirring. bvPLA2 was added last to give a final concentration of 128 nM, which corresponds to an average of six enzymes per vesicle. After addition of 67 μM $CaCl_2$, the reaction mixture was incubated for 15 min to allow hydrolysis of all of the available substrate as monitored with the pH stat. The quenching reaction was initiated by adding sodium dithionite from a stock solution [1.44 M, freshly prepared in 0.5 M Na_2CO_3 (pH 11) buffer saturated with nitrogen, stored at 0 °C for no more than 1 h] to a final concentration of 5.6 mM. The time-dependent decrease in fluorescence at 535 nm was recorded for 600 s

on an SLM-Aminco AB-2 spectrophotometer. Excitation was at 460 nm with both slit widths at 4 nm.

Substrate specificity studies using the competitive dual-radiolabel approach were carried out as described (Ghomashchi et al., 1991a). Briefly, the phospholipids used were [^{14}C]PAPC (50 Ci/mol, NEN), [^{3}H]DPPC (50 Ci/mmol, NEN), and [^{3}H]SAPC [400 Ci/mol, prepared as described (Hanel et al., 1993)]. Additional phospholipids were prepared by phospholipase D-catalyzed transphosphatidylation (Ghomashchi et al., 1991a; Hanel et al., 1993): [^{14}C]PAPA (2 Ci/mol), [^{14}C]PAPS (2 Ci/mol), and [^{14}C]PAPE (2 Ci/mol). Reaction mixtures (4 mL) contained 0.6 mg of DMPM, ^{3}H- and ^{14}C-labeled phospholipids [in approximately the amount given in Ghomashchi et al. (1991a)], 2.5 mM $CaCl_2$, 1 mM NaCl, and 20 μg of polymyxin B.

Determination of the Interfacial Equilibrium Dissociation Constants. Detailed theoretical and experimental protocols for the determination of the equilibrium constant for the dissociation of a ligand from the E*•L complex bound to the surface of a neutral diluent have been previously described (Jain et al., 1991d; Yu et al., 1993), and modifications required for analysis of bvPLA2 are developed in the Appendix. Briefly, alkylation of the active site histidine residue of bvPLA2 by PNBr (Sigma) in the presence or absence of ligand was carried out in a 0.03 mL reaction mixture at 22 °C in a 6 × 50 mm borosilicate tube containing 0.4 μM bvPLA2, 50 mM sodium cacodylate buffer (pH 7.3), and 2 mM PNBr, with or without 1.65 mM D-LPC, and with or without 0.5 mM $CaCl_2$. At various times, an aliquot containing 0.4 pmol of enzyme was diluted into the assay mixture at 22 °C containing a sonicated dispersion of 1 μg of 1-hexadecanoyl-2-(1-pyrenedecanoyl)-*sn*-glycero-3-phosphomethanol (Molecular Probes) and 250 μg of fatty acid-free bovine serum albumin (Sigma A-9647) in 1.5 mL of 100 mM NaCl, 0.25 mM $CaCl_2$, and 50 mM Tris-HCl at pH 8.5. The change in emission fluorescence at 395 nm (excitation at 345 nm with both slit widths at 4 nm) was continuously monitored with an SLM 4800S spectrofluorimeter. Prior to the addition of enzyme, the assay mixture was pre-equilibrated for 2−3 min until a stable, low-drift baseline was obtained.

Residual bvPLA2 activity in the inactivation mixture was determined from the initial rate of hydrolysis observed in the fluorimetric assay. The inactivation profile was biphasic; a fast phase (half-time of ≈ 1−3 min) and a slow phase (half-time of 25−500 min, depending on the presence of the active site ligand) were seen. It appears that the alkylation of a residue other than the active site histidine was occurring during the fast phase since it is the rate of alkylation during the slow phase that is decreased in the presence of an active site-directed ligand. Thus, residual bvPLA2 activity vs time of incubation with PNBr was fitted to a double-exponential equation by nonlinear regression to obtain the half-time for inactivation during the slow phase. In the absence of PNBr, with 1.65 mM D-LPC and 0.5 mM Ca^{2+}, the residual activity remains constant for more than 10 h.

Values of K_{Ca} and K_{Ca}*(ND) were obtained by monitoring the decrease in tryptophan fluorescence emission from bvPLA2 in aqueous solution or bound to D-LPC micelles, respectively, as a function of the Ca^{2+} concentration.

Amino acid analysis of bvPLA2 treated with or without PNBr was carried out. Enzyme (4 μM) in 2 mL of inactivation buffer was treated with or without 2 mM PNBr for 80 min. The reactions were quenched by the addition of 130 μL of 1 N HCl. The sample with PNBr was loaded onto a 0.5 mL bed of SP-Sephadex (Pharmacia, equilibrated with 10 mM MES at pH 5.0) in a 1 mL disposable syringe. The syringe was centrifuged at about 2500 rpm for 30 s. Five milliliters of MES buffer was applied to the column, which was spun again, and this washing procedure was repeated two more times (this removes PNBr). Enzyme was eluted by washing the column with 3 mL of MES buffer containing 1 M NaCl. The bvPLA2 in the eluant was purified by reverse phase HPLC as described previously (Ghomashchi et al., 1991b). Samples were concentrated to dryness in a Speed-Vac apparatus (Savant Instruments), and amino acid analysis was obtained commercially (BioSynthesis Inc.) using norleucine as an internal standard. Data are given as the moles of amino acid per enzyme ± standard deviation (three runs).

Vesicle Binding Studies. Binding of bvPLA2 to vesicles was determined by fluorescence energy transfer from tryptophan residues on the enzyme to the labeled head group of dansyl-DTPE. Stock solutions of DTPC, DTPM, and dansyl-DTPE in 2:1 $CHCl_3$/CH_3OH were mixed to give either 98:2 DTPC:dansyl-DTPE or 78:20:2 DTPC/DTPM/dansyl-DTPE (mole ratios), and the solvent was removed at room temperature by evaporation under a stream of argon, followed by evaporation *in vacuo* for 30 min. The lipid film was hydrated in 10 mM Tris at pH 8.0 to give a final lipid concentration of 40 μM and sonicated for 2−5 min, when a clear suspension of vesicles was obtained. One milliliter of vesicle suspension was transferred to a 1 cm × 1 cm cuvette, and the Ca^{2+} concentration was adjusted to 1 mM by adding 1 μL of 1 M $CaCl_2$. Fluorescence emission spectra from 300 to 650 nm were obtained at 23−24 °C using a Perkin-Elmer 650−10S fluorescence spectrophotometer (excitation at 292 nm, slit widths of 5 nm). Aliquots of bvPLA2 were added, and the sample was incubated for 2−3 min before obtaining another spectrum. Data are expressed as $R = (F - F_0)/F_0$, where F is the fluorescence at 506 nm and F_0 is the background (no bvPLA2) fluorescence at the same wavelength.

RESULTS

bvPLA2 Operates on DMPM Vesicles in the Scooting Mode. As previously described in detail, the analysis of the reaction progress for interfacial catalysis in the scooting mode permits the experimental determination of the kinetic constants (Figure 1) (Berg et al., 1991; Jain et al., 1995). As shown by the results below, in the scooting mode, bvPLA2, like type I and II PLA2s (Gelb et al., 1995; Jain et al., 1995), remains tightly bound to the vesicle surface, and lipolysis occurs in a processive fashion in which all of the substrate in the outer monolayer of enzyme-containing vesicles is hydrolyzed without desorption of enzyme from the interface. Since type I and II PLA2s bind several orders of magnitude tighter to anionic vesicles than to charge neutral vesicles and operate in the scooting mode on the former but not on the latter (Gelb et al., 1995; Jain et al., 1995), the vesicle binding properties of bvPLA2 were studied as a prelude to the kinetic studies. Binding of bvPLA2 to vesicles was assessed using fluorescence energy transfer from tryptophan residues on the enzyme to the dansyl-labeled head group of dansyl-DTPE incorporated into vesicles (Figure 2). Binding of bvPLA2 to anionic DTPC/DTPM/dansyl-DTPE (78:20:2) vesicles is

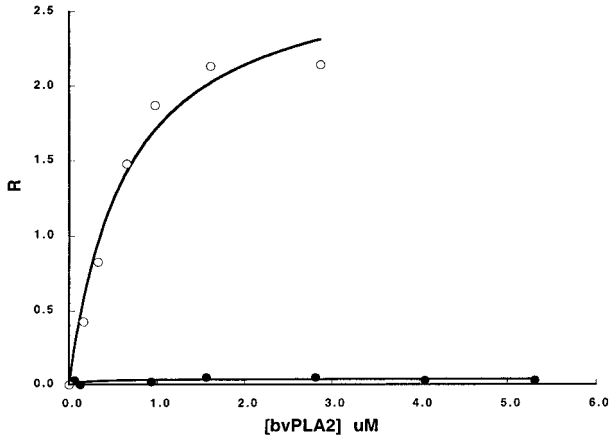

FIGURE 2: Binding of bvPLA2 to phospholipid vesicles. Binding of bvPLA2 to vesicles of DTPC/DTPM/dansyl-DTPE (78:20:2, 40 μM total phospholipid) (open circles) or to vesicles of DTPC/dansyl-DTPE (98:2, 100 μM total phospholipid) (closed circles) is shown. Binding was measured by fluorescence energy transfer from tryptophan residues on bvPLA2 to the dansyl fluorophore (R is defined in Materials and Methods). Excitation was at 292 nm; emission was at 495 nm, and slit widths were 5 nm.

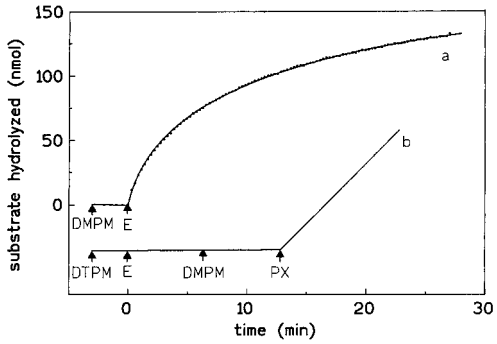

FIGURE 3: Hydrolysis of DMPM vesicles by bvPLA2. (a) Reaction progress curve for the hydrolysis of 0.3 mM DMPM vesicles by 0.2 μg of bvPLA2 in 4 mL of 0.5 mM $CaCl_2$ and 1 mM NaCl at 22 °C and pH 8.0. The line through the dots is the fitted curve according to eq 3. (b) bvPLA2 (0.2 μg) was added to 0.08 mM DTPM vesicles in a 4 mL reaction mixture. DMPM was added after 7 min to 0.3 mM, and no reaction was seen, which indicates that the enzyme is trapped on the DTPM vesicles. The reaction started immediately after the addition of 20 μg of polymyxin B (PX), which causes intervesicle phospholipid transfer without fusion. The lines through the data points are shown, and there was no deviation from linearity.

too tight to permit an accurate estimate of the binding constant. This is because the dissociation constant is much less than 1 μM phospholipid, and energy transfer experiments are not sensitive enough to work at such low lipid concentrations. No binding of bvPLA2 to vesicles without DTPM (DTPC/dansyl-DTPE, 98:2) was seen even when the total lipid concentration was 100 μM (Figure 2).

Once the fact that bvPLA2 binds tightly to anionic vesicles was established, kinetic studies to probe the reversibility of binding were carried out. The following experimental observations establish that bvPLA2 binds irreversibly to DMPM vesicles and operates in the scooting mode. (1) The results shown in Figure 3 (bottom) establish that DMPM vesicles added to a solution of bvPLA2 prebound to vesicles of the nonhydrolyzable phospholipid DTPM are not hydrolyzed. That the enzyme bound to DTPM vesicles is still active is shown by the fact that hydrolysis occurs immediately after addition of polymyxin B (Figure 3b) which allows DMPM to transfer to enzyme-containing DTPM vesicles as established previously (Cajal et al., 1995, 1996; Jain et al., 1991b). Furthermore, the addition of high calcium (2.5 mM) causes enzyme-containing DTPM vesicles to fuse with DMPM vesicles (Jain et al., 1991b), and this leads to immediate hydrolysis of DMPM (not shown). Enzyme is also irreversibly bound to anionic vesicles made of a 1:1 mixture of the products of DMPM hydrolysis (myristic acid and 1-myristoyl-*sn*-glycero-3-phosphomethanol) (not shown). (2) Addition of DTPM vesicles to a reaction of bvPLA2 on DMPM vesicles in the absence of lipid transfer agents does not alter the reaction progress (not shown), which shows that bvPLA2 bound to DMPM vesicles is not able to transfer to DTPM vesicles. (3) When DMPM vesicles containing a trace amount of [^{3}H]DPPC (4000 cpm, 2×10^{-7} mole fraction) are added to a reaction mixture containing bvPLA2 prebound to DMPM vesicles without radioactive lipid, the release of radiolabeled palmitic acid after 10 min is 3% of that observed 10 min after enzyme is added to DMPM/[^{3}H]-DPPC vesicles. This proves that bvPLA2 is irreversibly bound to DMPM vesicles. (4) Fluorescence energy transfer between tryptophan residues of bvPLA2 and dansyl-DTPE present in DTPM vesicles to which the enzyme is bound does not diminish when DMPM vesicles without dansyl-DTPE are added (not shown). (5) Under conditions in which the vesicle:enzyme ratio is greater than 5 or so, vesicles will contain at most one enzyme [according to the Poisson distribution for the random binding of enzyme to vesicles (Berg et al., 1991)]. Under these conditions, if bvPLA2 bound to a DMPM vesicle hydrolyzes all of the substrate in the outer layer of a vesicle (there are N_S phospholipid molecules in the outer layer of a vesicle), the total moles of product at the end of the reaction, P_{max}, is given by eq 1 (Berg et al., 1991):

$$P_{max} = C_E N_S \quad (1)$$

Here, C_E is the total moles of enzyme. It has previously been shown that, with bvPLA2 as well as with several other secreted PLA2s, the observed P_{max} is proportional to the amount of enzyme as long as the vesicle:enzyme ratio is greater than 5 or so (Jain et al., 1991a). Furthermore, the value of N_S obtained from eq 1 using bvPLA2/DMPM agrees with the value of N_S calculated from the experimentally determined vesicle size (Jain et al., 1991a; Berg et al., 1991).

Direct proof that bvPLA2 does not induce transbilayer movement of DMPM from the inner monolayer of the vesicle to the outer monolayer (flip-flop) is shown in Figure 4. Addition of dithionite to vesicles of DMPM/POPC (7:3) containing 0.6% *N*-(7-nitro-2−1,3-benzoxadiazol-4-yl)dioleoylphosphatidylethanolamine in the absence of bvPLA2 results in a decrease of fluorescence of about 70% (with multilamellar vesicles, only 8% of the fluorescence is lost in less than 100 s). This is expected if only the fluorophore in the outer monolayer of the vesicles is reduced. Reduction starts immediately after the addition of dithionite, and the time course has two components: a fast reaction (half-time $\sim$ 15 s) which is complete within 100 s and a parallel slow phase. The fast phase is due to reduction of the fluorophore in the outer monolayer of the vesicles. The slower phase is attributed to leakage of dithionite into the inner aqueous compartment of the vesicle with subsequent reduction of fluorophore in the inner monolayer. Several controls support this hypothesis. If vesicles are disrupted with deoxycholate prior to addition of dithionite, all of the fluorescence is lost in less than 100 s. The possibility that dithionite is exhausted

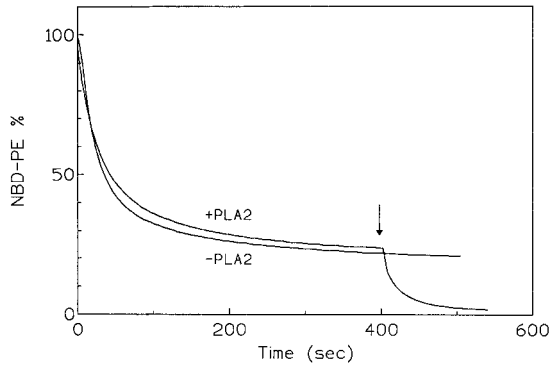

FIGURE 4: Time course for loss of fluorescence of *N*-(7-nitro-2−1,3-benzoxadiazol-4-yl)dioleoylphosphatidylethanolamine (0.6% in POPC/DMPM vesicles) by dithionite added to the aqueous phase. The *y*-axis gives the fluorescence from the NBD group as a percentage of the initial fluorescence measured before the addition of dithionite. Dithionite (5.6 mM) was added at time zero to a suspension of vesicles (110 μM) in 10 mM Tris and 0.67 mM $CaCl_2$ at pH 8.0 with or without bvPLA2 (128 nM), and the NBD fluorescence was measured as a function of time (*x*-axis). For the +PLA2 curve, the outer monolayer of the vesicles was hydrolyzed with bvPLA2 prior to the addition of dithionite (see Materials and Methods). At the end of the reaction, deoxycholate was added to a final concentration of 2.2 mM (marked with an arrow), allowing reduction of the inner monolayer lipid.

over the time course of the experiment is ruled out by the observation that adding a second portion of dithionite only leads to a slight increase in the rate of the slow phase. DMPM/POPC covesicles were used because vesicles of pure DMPM are considerably more leaky toward dithionite. If dithionite is added to vesicles that have been previously hydrolyzed by adding bvPLA2 and $CaCl_2$ until the reaction ceases (monitored in the pH stat), the same rapid decrease in fluorescence as that seen in the absence of enzymatic hydrolysis was observed (Figure 4). This indicates that flip-flop of the fluorescent phospholipid from the inner monolayer of the vesicle to the outer monolayer does not occur. This supports the result that bvPLA2 does not hydrolyze phospholipids present in the inner monolayer. Furthermore, the results also strongly suggest that the products of bvPLA2 hydrolysis do not move to the inner monolayer since such movement would be accompanied by a balancing movement of fluorescent phospholipid to the outer monolayer, which does not occur. Additional evidence that DMPM vesicles hydrolyzed by bvPLA2 remain intact comes from the observation that vesicles loaded with a mixture of 1-aminonapthalene-3,6,8-trisulfonic acid and *N*,*N*′-*p*-xylenebis(pyridinium bromide) do not release these spectral probes as monitored by the published method (Ellens et al., 1985).

Kinetics of bvPLA2 Acting on DMPM Vesicles in the Scooting Mode. Once the fact that bvPLA2 acts on DMPM vesicles in the scooting mode was established, the analysis of the reaction progress curve was carried out. The Michaelis−Menten equation for scooting mode hydrolysis of vesicles is given by eq 2 (Berg et al., 1991):

$$\nu_0 = \frac{k_{cat}}{X_S + K_M^*} \tag{2}$$

Here, ν_o is the initial velocity per enzyme, K_M* the interfacial Michaelis constant (units of mole fraction), and k_{cat} the interfacial maximal turnover number. The integrated interfacial Michaelis−Menten equation is given by eq 3 (Berg et al., 1991):

$$k_i t = -\ln\left(1 - \frac{P_t}{P_{max}}\right) + \left(\frac{k_i N_S}{\nu_0} - 1\right)\frac{P_t}{P_{max}} \tag{3}$$

Here, P_t and P_{max} are the moles of product formed at time t and at time infinity, respectively. $N_S k_i$ is given by eq 4 (Berg et al., 1991):

$$N_S k_i = \frac{k_{cat}}{K_M^*\left(1 + \frac{1}{K_P^*}\right)} \tag{4}$$

Here, K_P* is the equilibrium constant for the dissociation of reaction products from the E*·P complex.

As shown in Figure 3a, within the constraints described previously (Berg et al., 1991), the entire progress curve for the hydrolysis of DMPM vesicles in the scooting mode is analytically described by eq 3. As shown elsewhere (Berg et al., 1991), the parameters ν_o and $N_S k_i$ are obtained from such a curve. Values of ν_o and $N_S k_i$ for the action of bvPLA2 on DMPM vesicles are listed in Table 1 along with the corresponding values for PLA2s from porcine pancreas (Berg et al., 1991; Jain et al., 1991d) and human synovial fluid (nonpancreatic secreted PLA2) (Bayburt et al., 1993).

Agents which promote rapid fusion of DMPM vesicles, such as high concentrations of Ca^{2+} (Jain et al., 1986), or which promote direct intervesicle phospholipid transfer without fusion, such as polymyxin B (Cajal et al., 1996; Jain et al., 1991b), cause rapid substrate replenishment in enzyme-containing vesicles. Under such conditions, the reaction progress curve takes on a prolonged initial linear shape as the substrate is rapidly replenished in enzyme-containing vesicles. This maintains the mole fraction of substrate "seen" by the enzyme near 1 such that the ν_o is obtained from the zero-order phase of the reaction progress curve. The value of $\nu_o = 98\ s^{-1}$ is obtained under these conditions, and this agrees well with $\nu_o = 90\ s^{-1}$ obtained by fitting the data in Figure 3 to eq 2.

Interfacial Enzyme−Ligand Dissociation Equilibrium Constants. *(i) An Imperfect Neutral Diluent of bvPLA2*. Determination of the interfacial dissociation constants for ligands bound to the enzyme at the interface requires the use of a neutral diluent (Jain et al., 1991d). A neutral diluent is an amphiphile that forms aggregates to which PLA2 binds, but the amphiphile does not occupy the active site of the bound enzyme. Thus, neutral diluents, when incorporated into phospholipid vesicles, are useful as two-dimensional solvents for decreasing the mole fraction of substrate at the interface. Neutral diluents for bvPLA2 are identified by monitoring the rate of alkylation of the active site histidine residue by phenacyl bromides (Jain et al., 1991d). If the enzyme binds to the aggregate of the neutral diluent and if the rate of active site alkylation of the bound enzyme is the same as for the enzyme in the aqueous phase, then the active site is not occupied by a molecule of the aggregate. Ligands that bind in the active site of an enzyme bound to a neutral diluent confer protection from alkylation to the enzyme, and this effect is used to measure the equilibrium constant for the dissociation of the E*·ligand complex.

To find an agent that is a neutral diluent for bvPLA2, several amphiphiles were tested at a mole fraction of 0.1−

Table 1: Rate and Equilibrium Parameters for the Action of Secreted PLA2s in the Scooting Mode on DMPM Vesicles

	value[a]		
parameter (units)	bvPLA2	porcine pancreatic PLA2[b]	human nonpancreatic secreted PLA2[c]
ν_0 (s^{-1})	90	320	100
$N_S k_i$ (s^{-1})	12	35	13
k_{cat} (s^{-1})	126 (eq 2)	400	>200
K_M*	0.29 (eqs 2 & 4), 0.26 (eq 8), 0.4−0.7 (eq 9), 0.36 (eq 9, $K_I^* = K_{ND}^*$), and 0.34 (eq 10 with MJ33)	0.3−0.67	1.5−4
K_{Ca} (mM)	0.32 (Figure 6)	0.35	1.6
K_{Ca}* (mM)	0.53 (eq 6)	0.25	1.2
K_{Ca}*(ND) (mM)	0.17 (eq 5), 0.07 (Figure 6)		
K_{Ca}*(S) (mM)	0.11 (ν_o vs $[Ca^{2+}]$)	0.1	0.95
K_I* (DTPM)	0.032 (eqs A4 and A5)	0.017	>0.2
K_I* (DTPC)	> 1 (eqs A4 and A5)	0.065	0.6
K_P* (products of DMPM hydrolysis)	0.03 (eqs A4 and A5)	0.03	0.12
K_I* (MJ33)	0.0025 (eqs A4 and A5)	0.0014	0.14
K_I* (MG14)	0.0030 (eqs A4 and A5)	0.0011	0.03
$n_I(50)$	0.05 ($N_s k_i$ vs X_I)	0.028	
$X_I(50)$ (MJ33)	0.006 (ν_0 vs X_I)	0.006	0.19
$X_I(50)$ (MG14)	0.011 (ν_0 vs X_I)	0.0034	0.052
K_{ND}*	0.47 (D-LPC) (eq A8)	>4 (1-palmitoyl-2-deoxy-*sn*-glycero-3-phosphocholine)	>1 (hexadecylphosphorylcholine)
k_I^*/k_0^*	0.13 (eq 7, average for all inhibitors)	<0.05	<0.05
relative k_{cat}/K_M*			
PAPS vs SAPC	1.09	no data	3.6 (DMPS vs SAPC)
PAPE vs SAPC	0.83	1.2 (DPPE vs DPPC)	1.09 (DPPE vs DPPC)
PAPA vs SAPC	0.57	3.0 (DPPA vs DPPC)	1.49 (DPPA vs DPPC)
PAPC vs DPPC	1.13	0.59	0.53

[a] The errors of all measured quantitites are ±10%, and the errors in the parameters listed in this table, which are derived from two measured quantities, are ±30%. Values of two-dimensional equilibrium and Michaelis constants marked with an asterisk (i.e. K_M*), $X_I(50)$, and $n_I(50)$ are expressed as mole fraction. [b] Ghomashchi et al. (1991a), Berg et al. (1991), and Jain et al. (1991d). [c] Bayburt, et al. (1993).

Table 2: Half-Times for Inactivation of bvPLA2 by PNBr

additive	half-time (min) of the fast phase	half-time (min) of the slow phase
11 mM EGTA (or 0.2 mM BAPTA)	0.6	23.5
0.5 mM $CaCl_2$	0.7	23.9
10 mM $CaCl_2$	0.8	22
11 mM EGTA (or 0.2 mM BAPTA) + 1.65 mM D-LPC	3	56
0.5 mM $CaCl_2$ + 1.65 mM D-LPC	3	104
10 mM $CaCl_2$ + 1.65 mM D-LPC	3	135
0.5 mM $CaCl_2$ + 5 mM hexadecylphosphorylcholine	3	144
0.5 mM $CaCl_2$ + 1.65 mM 1-palmitoyl-2-deoxy-*sn*-glycero-3-phosphocholine	3	418
0.5 mM $CaCl_2$ + 1.65 mM *rac*-2-hexadecyl-*sn*-glycero-3-phosphocholine	3	263
0.5 mM $CaCl_2$ + 1.65 mM D-LPC + 0.7 mM MJ33	3	286
9 mM EGTA + 1 mM bis-PC		300

0.3 in DMPM vesicles for their ability to inhibit the enzyme, presumably by binding to its active site, but not by disrupting the vesicles. Some of the amphiphiles that gave the least amount of inhibition were tested for their effect on the half-time for alkylation of bvPLA2 by PNBr (Table 2). Of these, D-LPC produced a relatively small increase in the alkylation half-time (2.4-fold). D-LPC was also found to be a weak inhibitor of bvPLA2-catalyzed hydrolysis of DMPM in the scooting mode; the mole fraction of D-LPC in DMPM vesicles that is required to decrease ν_o by 2-fold is 0.53. Thus, D-LPC is not a perfect neutral diluent for bvPLA2 in that it has measurable affinity for the active site of E*. The amphiphiles 1-palmitoyl-2-deoxy-*sn*-glycero-3-phosphocholine and *rac*-2-hexadecyl-*sn*-glycero-3-phosphocholine that are effective neutral diluents of the PLA2 from porcine pancreas (Jain et al., 1991d) and hexadecylphosphorylcholine which is a neutral diluent for the PLA2 from human synovial fluid (Bayburt et al., 1993) are not neutral diluents for bvPLA2, nor is bis-PC (Table 2).

bvPLA2 binds to D-LPC micelles in the absence of Ca^{2+} as shown by a 30% increase in tryptophan fluorescence emission intensity at 337 nm when increasing amounts of D-LPC are added to a solution of enzyme. The change in intensity showed a hyperbolic dependence on the concentration of D-LPC with an apparent dissociation constant of 0.1 mM (not shown). Thus, all of the enzyme is bound to D-LPC micelles under the conditions described in Materials and Methods (1.65 mM D-LPC).

The time course of inactivation of bvPLA2 in solution or bound to D-LPC micelles by PNBr has two components (Figure 5). Within the first 1−3 min, the percent of enzymatic activity drops to about 40%, and then the enzyme becomes fully inactivated over a slower time period. This data could be adequately fitted to a double-exponential equation. As summarized in Table 2, the rapid phase is only slightly affected by the presence of ligands that bind to the enzyme's active site, whereas the slow phase is sensitive to the nature and mole fraction of active site ligands. Thus, in the following discussion, the term "half-time" for alkylation refers to the slow phase inactivation half-time.

The following evidence strongly suggests that the slow phase of inactivation is due to PNBr alkylation of the active

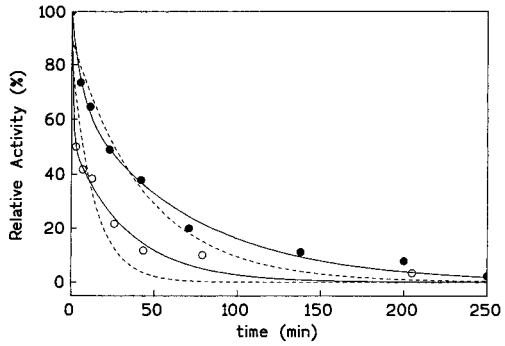

FIGURE 5: PNBr inactivation curves for 0.4 μM bvPLA2 in 0.1 M cacodylate buffer, 0.1 M NaCl, 11 mM EGTA, and 2 mM PNBr at pH 7.3 and 22 °C in the absence (open circles) or presence (closed circles) of 1.65 mM D-LPC. The data points were fitted by nonlinear regression to a single (dashed line)- or to a double (solid line)-exponential decay equation.

site histidine. Amino acid analysis of wild-type recombinant bvPLA2 before and after an 80 min treatment with PNBr indicates that 2.1 ± 0.7 histidines are lost after alkylation, and loss of all other amino acids is ≤0.30. When this experiment is repeated with the mutant in which the active site histidine is changed to glutamine (H34Q), the loss of histidine after PNBr treatment is 0.9 ± 0.4, and the loss of other amino acids is ≤0.33. These results show that PNBr only alkylates histidine and that at least one of the alkylated histidines is the active site histidine-34. That the slow phase of inactivation is due to histidine-34 alkylation is based on the observation that the slow phase rate of histidine alkylation is sensitive to pH, and a pK_a of 5.3 is obtained from the titration (Annand et al., 1996). The pK_a of this histidine is shifted to 4.5 for the mutant in which the asparate that hydrogen bonds to histidine-34, aspartate-64, is changed to glutamine. This pK_a shift is expected when the negatively charged aspartate is replaced with the neutral asparagine.

On the basis of all of these features of the kinetics of bvPLA2 inactivation by PNBr in the presence and absence of D-LPC, the equations previously described for determining interfacial equilibrium dissociation constants for secreted PLA2·ligand complexes by the protection from alkylation method (Jain et al., 1991d) require additional components (Appendix). As will become apparent below, an additional complexity with bvPLA2 exists because binding of ligands to the active site does not fully protect the enzyme from alkylation; the bvPLA2·ligand complex is only about 80% protected from alkylation, which is in marked contrast to pancreatic and synovial fluid PLA2s, which are nearly fully protected in complexes with active site ligands (Bayburt et al., 1993; Jain et al., 1991d).

(ii) The Effect of Calcium. As is the case with other secreted PLA2s, Ca^{2+} is an obligatory catalytic cofactor for interfacial catalysis by bvPLA2. One unusual feature was noted with bvPLA2. The half-times for PNBr alkylation of bvPLA2 in the aqueous phase in the presence and absence of Ca^{2+} were the same (Table 2). Thus, active site-bound Ca^{2+} does not protect the catalytic histidine from alkylation, which is in marked contrast to other secreted PLA2s (Bayburt et al., 1993; Jain et al., 1991d). Evidence for the binding of Ca^{2+} to bvPLA2 was obtained from the decrease in the enzyme's tryptophan emission. Fitting the data (Figure 6) to the equation for a rectangular hyperbola gives a value for the dissociation constant for E·Ca^{2+} in the aqueous phase (K_{Ca}) of 0.32 mM.

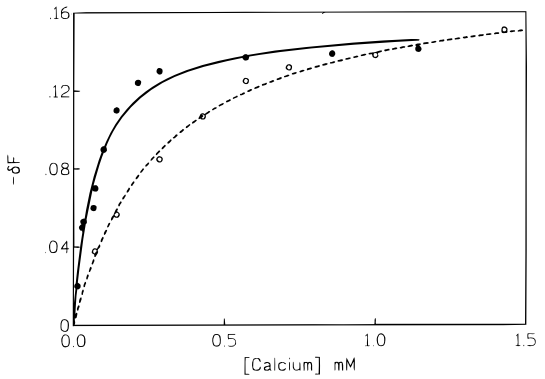

FIGURE 6: Decrease in fluorescence emission intensity of 4 μM bvPLA2 alone (open circles) or in the presence of 1.6 mM D-LPC (filled circles) as a function of the Ca^{2+} concentration in 10 mM Tris at pH 8.0. Emission was monitored at 336 nm with excitation at 292 nm. The lines are the fit of the data to the equation for a rectangular hyperbola. Data at high Ca^{2+} concentrations (up to 10 mM) are not shown.

In the absence of Ca^{2+}, the alkylation half-time increases 2.4-fold when 1.65 mM D-LPC is present (Table 2), and there is no further change in the half-time if the amount of D-LPC is increased further. These results confirm the spectroscopic results described above showing that all of the enzyme is bound to micelles in the presence of 1.65 mM D-LPC. On the basis of the arguments presented in the Discussion, it is unlikely that D-LPC occupies the active site of bvPLA2 in the absence of Ca^{2+}. Thus, in subsequent discussions, this form of the enzyme will be referred to as E*.

As shown in Table 2, the alkylation half-time for bvPLA2 bound to D-LPC micelles increases from 56 to 104 or 135 min in the presence of 0.5 or 10 mM Ca^{2+}, respectively. Since the binding of Ca^{2+} to bvPLA2 in the aqueous phase does not change the half-time for alkylation, it is very likely that this is true for enzyme bound to D-LPC micelles. Thus, the increase in the half-time when Ca^{2+} is added to bvPLA2 in the presence of D-LPC is most likely due to Ca^{2+}-promoted binding of D-LPC in the enzyme's active site to give the complex E*·Ca^{2+}·D-LPC. Many active site inhibitors of secreted PLA2s require Ca^{2+} for enzyme binding, which is consistent with the fact that the *sn*-3 phosphate of phospholipid analogs binds directly to this metal (Scott & Sigler, 1994). The consequence of this Ca^{2+}-promoted ligand binding on the half-times for histidine alkylation has been previously described (Yu et al., 1993), but a slightly modified equation is needed in the present case because D-LPC has finite affinity for the E*·Ca^{2+} complex, and eq 5 (derived in the Appendix) applies:

$$\frac{1}{1-\dfrac{t_0^*}{t_{Ca}^*}} = \frac{1+\dfrac{K_{Ca}^*(\mathrm{ND})}{[Ca^{2+}]}}{1-\dfrac{k_{ND}^*}{k_0^*}}(1+K_{ND}^*) \qquad (5)$$

This equation is similar to that published previously, but it contains an extra factor (1 + K_{ND}*), where K_{ND}* is the equilibrium constant for the dissociation of D-LPC from the E*·Ca^{2+}·D-LPC complex (note $K_{ND}^* \gg 1$ for a perfect neutral diluent). Here, t_0* and t_{Ca}* are the half-times for alkylation of bvPLA2 bound to D-LPC micelles in the absence of Ca^{2+} or in the presence of Ca^{2+} at concentration

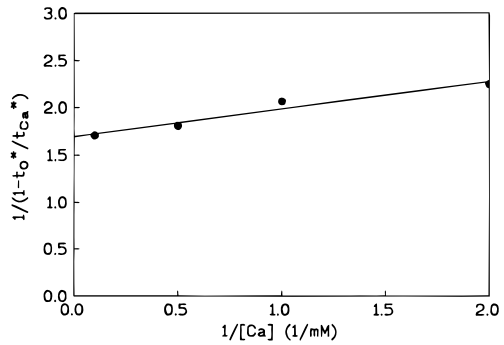

FIGURE 7: Effect of Ca^{2+} on the half-time for alkylation of bvPLA2 bound to 1.65 mM D-LPC micelles by PNBr. Other conditions are given in the legend to Figure 5.

$[Ca^{2+}]$, respectively, and k_{ND}* and k_0* are the rate constants for alkylation of E*·Ca^{2+}·D-LPC or E* (and E*·Ca^{2+}), respectively (note that rate constants refer to single enzyme species, but half-times are measured in the presence of a mixture of enzyme species). K_{Ca}*(ND) is the effective dissociation constant for Ca^{2+} in the presence of D-LPC. A plot of the left term in eq 5 vs the reciprocal of the Ca^{2+} concentration is shown in Figure 7. From the *x*-intercept, $-1/K_{Ca}$*(ND), K_{Ca}*(ND) = 0.17 mM.

Binding of Ca^{2+} to bvPLA2 bound to D-LPC micelles was also monitored by tryptophan fluorescence, and K_{Ca}*(ND) = 0.07 mM was obtained from the data in Figure 6. This value agrees reasonably well with the value of 0.17 mM obtained by the protection method. It seems unlikely that the effect of Ca^{2+} on tryptophan fluorescence in the presence of D-LPC is due to the interaction of Ca^{2+} with the D-LPC interface which somehow leads to a change in tryptophan emission. This is based on the fact that aggregates of zwitterionic phosphocholine-containing amphiphiles have virtually no affinity for calcium in the low-millimolar range (Hauser et al., 1977). Also, the similar values of K_{Ca}*(ND) obtained from Figure 6 and from the protection method (*x*-intercept of Figure 7) suggest that the decrease in tryptophan emission induced by calcium is due to calcium-promoted binding of D-LPC in the active site. Recall that binding of bvPLA2 to D-LPC micelles results in a modest increase in fluorescence emission.

K_{Ca}*(ND) is related to the dissociation constant for the E*·Ca^{2+} complex, K_{Ca}*, and K_{ND}* by eq 6 (Yu et al., 1993).

$$K_{Ca}^*(\mathrm{ND}) = \frac{K_{Ca}^*}{\left(1 + \frac{1}{K_{ND}^*}\right)} \qquad (6)$$

K_{Ca}* = 0.53 mM using K_{ND}* = 0.47 mole fraction (determined as described in the next section) and K_{Ca}*(ND) = 0.17 mM (Figure 7). The fact that the values of K_{Ca}* and K_{Ca} (0.32 mM, Figure 6) are similar establishes that the affinities of E and E* for Ca^{2+} are similar, which also establishes that the binding of E to D-LPC micelles does not require Ca^{2+}. K_{Ca}*(ND) is less than K_{Ca}* as expected if Ca^{2+} promotes the binding of D-LPC in the active site of bvPLA2.

(iii) Effect of Inhibitors. The interaction of bvPLA2 bound to D-LPC micelles with a number of active site-directed inhibitors of secreted PLA2s, including D-LPC, was studied. Equation 5 above applies to the case where the only active site-directed inhibitor present in D-LPC micelles is D-LPC itself. The *y*-intercept of Figure 7 is $(1 + K_{ND}^*)/(1 - k_{ND}^*/k_0^*)$, and K_{ND}* = 0.47 using eq A8 in the Appendix in the following way, which makes used of active site-directed inhibitors present in D-LPC micelles in addition to D-LPC. The half-time for alkylation of bvPLA2 bound to D-LPC micelles in the presence of Ca^{2+} and an active site inhibitor other than D-LPC, t_I*, increases with increasing mole fraction of inhibitor in the micelles according to eq A4 of the Appendix. The *y*-intercepts obtained from plots of the type shown in Figure 7 and based on eq A4 for the inhibitors DTPM, DMPM reaction products (1:1 mixture of myristic acid and 1-myristoyl-*sn*-glycero-3-phosphomethanol), MJ33, and MG14 are in the range of 1.3−1.7 mole fraction (Table 3). In these plots, t_{ND}* = 136 min (Table 2) which is the half-time for inactivation of enzyme in the presence of saturating Ca^{2+} and in the absence of inhibitor I. The average value of the *y*-intercept of 1.48 is used in eq A6 to obtain k_I^*/k_{inact}^0 = 0.32. Here, k_I* is the rate constant for the alkylation of E*·Ca^{2+}·I by PNBr, and k_{inact}^0 is the rate constant for alkylation in the absence of I (i.e. for the E*·Ca^{2+}/E*·Ca^{2+}·D-LPC mixture). The fact that the *y*-intercept is not unity establishes the fact that the E*·Ca^{2+}·I is not fully protected from alkylation. This fact is independent of the value of K_{ND}* as long as $K_I^* \ll K_{ND}^*$, which is true for the inhibitors studied (shown below).

Table 3: Ligand-Afforded Protection of Alkylation of E*·Ca^{2+} by PNBr

additive present in D-LPC micelles[a]	*y*-intercept	k_I^*/k_0^*
no additive	1.7[b]	0.15[d]
DTPM	1.7[c]	0.18[e]
1:1 mixture of myristic acid and 1-myristoyllysophosphatidylmethanol	1.36[c]	0.10[e]
MJ33	1.55[c]	0.15[e]
MG14	1.3[c]	0.09[e]

[a] The concentrations of D-LPC and $CaCl_2$ are 1.65 and 0.5 mM, respectively. [b] From Figure 7. [c] From plots based on eqs A4-A6 of the Appendix. [d] From the *y*-intercept via eq 5. Here, the only inhibitor present is D-LPC, which has finite affinity for the active site of bvPLA2, and k_I* becomes k_{ND}*. [e] From the *y*-intercepts via eq 7.

Using the average value of the *y*-intercept of 1.48, t_{ND}* = 136 min, and t_0* = 56 min (both from Table 2), K_{ND}* = 0.47 mole fraction according to eq A8. This equation assumes that the rate constants for alkylation of E*·Ca^{2+}·D-LPC, k_{ND}*, and E*·Ca^{2+}·I, k_I*, are the same. The validity of this assumption and thus the accuracy of K_{ND}* are further addressed in the Discussion. With K_{ND}* = 0.47 mole fraction, one obtains k_{ND}^*/k_0^* = 0.15 from the *y*-intercept of the plot in Figure 7. Once again, the fact that this ratio is not zero implies that E*·Ca^{2+}·D-LPC, like E*·Ca^{2+}·I, is not fully protected from alkylation by PNBr.

With the value of K_{ND}* in hand, it is possible to obtain K_I*, which is the equilibrium constant for the dissociation of an active site inhibitor from the E*·Ca^{2+}·I complex. K_I* is obtained from the *x*-intercept of the plots based on eq A4 (described above) according to eq A5 and K_{ND}* = 0.47 mole fraction. K_I* values for the active site inhibitors studied are listed in Table 1. For all inhibitors, the condition $K_I^* \ll K_{ND}^*$ holds. K_I* for MJ33 in the absence of Ca^{2+} is $\gg$0.05 mole fraction, which demonstrates that the inhibitor binds to E*·Ca^{2+} much tighter than to E*, as is the case with other secreted PLA2s (Bayburt et al., 1993; Jain et al., 1991c; Yu et al., 1993).

By combination of eqs A3 and A6 of the Appendix and with the same assumption that $k_{ND}^* = k_I^*$, eq 7 is obtained.

$$\frac{k_1^*}{k_0^*} = \frac{y\text{-intercept} - 1}{y\text{-intercept} + \dfrac{1}{K_{ND}^*}} \tag{7}$$

The ratios of rate constants, k_I^*/k_0^*, for the ligands studied are listed in Table 3, and they are in the range of 0.09-0.18. Thus, all inhibitors studied when bound to $E^*{\cdot}Ca^{2+}$ protect the active site histidine from alkylation to about the same extent. Therefore, it is not unreasonable to assume that D-LPC also protects the active site to the same extent. The average ratio $k_I^*/k_0^* = 0.14$ (Table 3) can be compared to $k_{ND}^*/k_0^* = 0.15$ (from the *y*-intercept of eq 7). Thus, the assumption $k_{ND}^* = k_I^*$ is consistent as it should since this assumption was already used to obtain K_{ND}^*.

Interfacial Michaelis−Menten Constants. The value of K_M^* for DMPM substrate can be obtained by several methods which make use of the equilibrium dissociation constants obtained by the protection method (Berg et al., 1991). From the curve-fitting analysis of the progress curve (Figure 3a), one obtains the ratio $N_S k_i/\nu_o = 0.13$. This value along with $K_P^* = 0.03$ mole fraction (protection method) yields $K_M^* = 0.29$ mole fraction according to the ratio of eqs 4 and 2.

The value of $K_{Ca}^* = 0.53$ mM obtained by the protection method according to eq 6 is related to the apparent dissociation constant for Ca^{2+}, $K_{Ca}^*(S)$ (defined as the concentration of Ca^{2+} that gives half of the ν_o measured at saturating Ca^{2+}), according to eq 8 (Yu et al., 1993).

$$K_{Ca}^*(S) = \frac{K_{Ca}^*}{1 + \dfrac{1}{K_M^*}} \tag{8}$$

On the basis of this equation and the experimental value $K_{Ca}^*(S) = 0.11$ mM, $K_M^* = 0.26$.

Yet another way to determine K_M^* is to examine the effect of competitive inhibitors on ν_o for the hydrolysis of DMPM in the scooting mode. A competitive inhibitor of interfacial catalysis will reduce the initial velocity according to eq 9 (Jain et al., 1991d).

$$\frac{\nu_o^{\,o}}{\nu_o^{\,I}} = 1 + \left(\frac{1 + 1/K_I^*}{1 + 1/K_M^*}\right)\left(\frac{X_I}{1 - X_I}\right) \tag{9}$$

Here, $\nu_o^{\,o}$ and $\nu_o^{\,I}$ are the initial velocities per enzyme in the absence and presence of an inhibitor at mole fraction X_I, respectively. From plots based on eq 9 and the values of K_I^* for MG14 and MJ33 obtained by the protection method (Table 1), values of K_M^* of 0.4 and 0.7 mole fraction, respectively, are obtained from plots of the type shown in Figure 8. Figure 8 shows the plot based on eq 9 for D-LPC as the inhibitor present in DMPM vesicles. The value $K_M^* = 0.36$ mole fraction is obtained from the data and using $K_{ND}^* = K_I^* = 0.47$ obtained by the protection method.

MJ33 is a transition-state analog that binds to the active site of porcine pancreatic and human synovial fluid PLA2s (Bayburt et al., 1993; Jain et al., 1991c). Thus, it is reasonable to assume that MJ33 also binds to the active site of bvPLA2 and blocks substrate binding (competitive inhibition). Equation 10 is a relationship between the degree of inhibition by a competitive inhibitor and the constants K_M^* and K_P^* (Jain et al., 1991d).

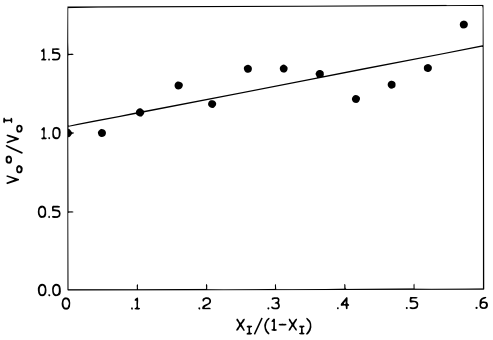

FIGURE 8: Plot of ν_o^o/ν_o^I vs $X_I/(1 - X_I)$ for the hydrolysis of 635 nmol of DMPM as vesicles in the presence of various mole fractions (X_I) of D-LPC. The reaction was initiated with 0.1−0.2 μg of bvPLA2 in a 4 mL reaction mixture containing 1 mM $CaCl_2$, 1 mM NaCl, and 20 μg of polymyxin B. A slope of 0.84 was obtained from linear regression analysis.

$$\frac{\dfrac{1}{X_I(50)} - 1}{\dfrac{1}{n_1(50)} - 1} = \frac{1 + \dfrac{1}{K_P^*}}{1 + \dfrac{1}{K_M^*}} = \frac{\nu_o}{N_S k_i} \tag{10}$$

Here, $X_I(50)$ and $n_I(50)$ are the mole fractions of inhibitor in DMPM vesicles that reduces ν_o and $N_S k_i$, respectively, by 2-fold. Equation 10 is true only if the inhibitor is competitive. From the values of $X_I(50)$ and $n_I(50)$ given in Table 1 for the inhibitor MJ33, the left side of eq 10 has a value of 8.7. This agrees reasonably well with values of $K_P^* = 0.03$ mole fraction and the average value of $K_M^* = 0.4$ mole fraction (determined by the multiple methods described above), and also with the value of 7.5 for the term on the right using the values of ν_o and $N_S k_i$ in Table 1. Equation 10 is also satisfied for MJ33 binding to porcine pancreatic and human synovial fluid PLA2s (Bayburt et al., 1993; Jain et al., 1991c).

Using the average value of $K_M^* = 0.4$ for DMPM obtained by all of these methods, a value of $k_{cat} = 126\ s^{-1}$ is obtained from eq 2 and $\nu_0 = 90\ s^{-1}$ (Table 1).

Substrate Specificity. The most meaningful way to determine the intrinsic substrate specificity of an interfacial enzyme is to examine its preferences for various substrates in the vesicle to which it is irreversibly bound (Ghomashchi et al., 1991a). Otherwise, the observed specificity may be more a reflection of how tightly the enzyme binds to vesicles of different phospholipid compositions. The ratio of k_{cat}/K_M^* values [the interfacial specificity constant (Ghomashchi et al., 1991a)] for the pairs of substrates tested in DMPM vesicles are listed in Table 1. The results show that bvPLA2 acting in the scooting mode on DMPM vesicles containing pairs of radiolabeled substrates does not significantly discriminate between phospholipids with polyunsaturated vs saturated *sn*-2 fatty acyl chains or between phospholipids with different polar head groups.

Comparison of Glycosylated and Nonglycosylated bv-PLA2. Naturally occurring bvPLA2 contains asparagine-linked carbohydrate (Kubelka et al., 1993; Shipolini et al., 1974). The X-ray structure of bvPLA2 shows that the carbohydrate is on the edge of the protein surface that is thought to contact the membrane (Scott et al., 1990), but it is not at all clear if the presence of carbohydrate perturbs the interfacial behavior of the enzyme. Thus, the interfacial

parameters of naturally occurring bvPLA2 and recombinant enzyme produced in *E. coli* (Dudler et al., 1992), which lacks carbohydrate, were compared. Within experimental error, no differences between glycosylated and nonglycosylated enzymes were noted in the reaction progress curves, the time course of inactivation by PNBr, protection from alkylation by the inhibitors MG14 and MJ33, and $X_I(50)$ values for these inhibitors.

DISCUSSION

It is apparent from the kinetic and equilibrium data in Table 1 for bvPLA2 (type III) and the previously reported kinetic and equilibrium data for pancreatic PLA2 (type I) and nonpancreactic secreted PLA2 (type II) that these evolutionarily different enzymes show remarkable functional similarity. This provides functional support for the view that, although the overall peptide backbone topology of bvPLA2 is very different from those of other secreted PLA2s, the active sites of all three enzymes are structurally similar (Scott & Sigler, 1994). All three enzymes are monomeric when operating on anionic vesicles in the scooting mode (Jain et al., 1991a). In all cases, Ca^{2+} is required for the binding of substrate and phospholipid analogs to the active site of enzyme at the interface ($E^* + S \rightarrow E^*{\cdot}S$) but not for the E to E* step [this paper and Bayburt et al. (1993) and Yu et al. (1993)]. The interfacial Michaelis constants, K_M^*, for bvPLA2 and its type I and II homologs are close to unity (Table 1), and thus, these enzymes operate in the presence of substrate concentrations that are near K_M^*. All three enzymes bind much tighter to anionic vesicles than to charge-neutral ones. bvPLA2, like pancreatic and nonpancreatic secreted PLA2s, has a collection of lysine and arginine residues that lie on the surface that is thought to contact the membrane, and these residues presumably allow electrostatic interaction with the anionic interface (Ramirez & Jain, 1991; Scott et al., 1994).

It is clear from studies of type I−III PLA2s that a single compound which is a neutral diluent for all three enzymes has not been found. Bis-PC was a hopeful neutral diluent candidate since it is difficult to imagine bis-PC entering the active site of PLA2 because this would involve pulling the polar head group on the opposite end of the phospholipid analog into the interior of the membrane. Perhaps some of the bis-PC is in a U-shaped configuration rather than one in which it spans the membrane, and perhaps the U-shaped bis-PC is flexible enough to at least partially enter the active site.

The most surprising behavior of bvPLA2 is that its active site histidine (His-34) is accessible to PNBr even when the active site contains calcium (no protection) or phospholipid analog (partial protection). On the basis of X-ray structures, the region of bvPLA2 where the polar head group of a bound phospholipid analog (MG14) sits is much more exposed to solvent than the analogous regions of pancreatic, nonpancreatic, and cobra venom secreted PLA2s (Scott & Sigler, 1994). This may allow PNBr to access the histidine by entering the active site near the head group of the enzyme-bound inhibitor. bvPLA2 contains a total of seven histidines. Amino acid analysis indicates that approximately two of them are being alkylated by PNBr. One of these is the catalytic histidine (His-34), and alkylation of this residue by PNBr occurs during the slow phase of inactivation. The fast phase of inactivation results in only a partial loss of enzymatic activity. This may be the result of alkylation of either His-11 or His-56; both residues lie at the entrance of the active site slot where phospholipid binds. The other histidines at positions 26, 48, 100, and 115 are on the surface of molecule that is opposite the putative membrane binding surface.

Identification of a neutral diluent is a critical step in characterizing interfacial equilibria. As shown in this study, it is possible to obtain interfacial enzyme·ligand equilibrium dissociation constants if the enzyme is bound to an imperfect neutral diluent such as D-LPC. As shown in the Appendix, with the assumption that $k_{ND}^* = k_I^*$, K_{ND}^* can be estimated. In the case of bvPLA2, the problem is compounded by the fact that the active site histidine is not fully protected when ligands bind to the active site. Under the assumption that $k_{ND}^* = k_I^*$, $K_{ND}^* = 0.47$. This appears to be a reasonable estimate of K_{ND}^* on the basis of the following arguments. First, the value of $K_M^* = 0.26-0.7$ for DMPM was obtained using a number of methods which rely on knowing the value of K_{ND}^*. It is clear from the progress curve in the absence of polymyxin B (Figure 3) that in small vesicles the velocity decreases rapidly even during the initial part of the curve. Thus, K_M^* is probably not <0.1 mole fraction; if it were, the progress curve would remain linear for a longer period of time. From the data in Figure 8, the initial velocity for hydrolysis of DMPM in the scooting mode is reduced about 30% when D-LPC is present at 0.3 mole fraction. According to eq 9, if $K_M^* > 0.1$ mole fraction, K_{ND}^* would be >0.1 mole fraction. For all four active site-directed inhibitors studied, DTPM, MJ33, MG14, and the products of DMPM hydrolysis, values of k_I^*/k_{inact}^0 are very similar and not equal to zero. This establishes not only that the $E^*{\cdot}Ca^{2+}{\cdot}I$ complexes can be alkylated by PNBr but also that the degree of protection of histidine-34 from alkylation by inhibitor is the same for all three inhibitors; this result is independent of the value of K_{ND}^*. It is thus reasonable to propose that binding of D-LPC to the active site of bvPLA2 provides a similar degree of protection from alkylation as do the four inhibitors, and thus, $k_{ND}^* \approx k_I^*$ is likely to be true. Finally, the value of K_{ND}^* is not very sensitive to the variation of k_{ND}^* with respect to k_I^*. For example, if $k_{ND}^* = 0.5k_I^*$, $K_{ND}^* = 0.6$; if $k_{ND}^* = 1.5k_I^*$, $K_{ND}^* = 0.37$, and an upper limit of $K_{ND}^* = 0.71$ is obtained if D-LPC fully protects ($k_{ND}^* = 0$). However, if D-LPC does not protect as well as the four inhibitors, K_{ND}^* would be much smaller than the estimate of 0.47. This seems very unlikely because the phosphorylcholine head group of D-LPC is considerably larger than the head groups of the four inhibitors (trifluoroethyl group of MJ33, the phosphoethanolamine group of MG14, and the phosphomethanol group of lysophosphatidylmethanol and DTPM).

There are very few experimental methods available for establishing neutral diluents of lipolytic enzymes. The protocol of using histidine alkylation by an active site-directed alkylating legend appears to be generally applicable to secreted PLA2s (Bayburt et al., 1993; Jain et al., 1991d). Although ligand binding to the active site of pancreatic PLA2 produces a distinct change in the UV spectrum of the protein that can be used to follow this type of ligand binding, it was only possible to establish this once a neutral diluent was discovered by the protection from alkylation method (Dupureur et al., 1992; Jain et al., 1993). Recently, Burke et al. (1995) published a different strategy for screening amphiphiles as possible neutral diluents. The method involves monitoring the hydrolysis of a radioactive phospholipid

substrate present in an aggregate of the candidate neutral diluent amphiphile as a function of the mole fraction of a non-radiolabeled competing substrate. The experiment is then repeated except that the radiolabel is now present in what was the non-radiolabeled substrate in the previous experiment. However, as shown in the Supporting Information, this method is mathematically flawed and thus cannot be used to establish a neutral diluent for interfacial enzymes.

ACKNOWLEDGMENT

We are grateful to Bruce Lennox for providing bis-PC.

APPENDIX

Analysis of the Equilibrium Dissociation Constant for the Complex bvPLA2·Inhibitor Bound to the Aggregate of an Imperfect Neutral Diluent. Consider a situation where the enzyme is bound to the surface of a neutral diluent (ND) which contains an inhibitor (I) at mole fraction X_I. If the ND is not completely neutral, it can bind to the active site with dissociation constant K_{ND}*. Similarly, the inhibitor binds with dissociation constant K_I*. As detailed in the main text, binding of both ND and I to the active site of bvPLA2 requires Ca^{2+}, and thus, the enzyme species was considered to have calcium bound at the active site. The strength of this binding can be determined by studying the protection from enzyme inactivation afforded by ND and I.

$$\begin{array}{l} E^*\cdot Ca^{2+}\cdot ND \xrightarrow{k_{ND}^*} \\ K_{ND}^* \uparrow\downarrow \\ E^*\cdot Ca^{2+} \xrightarrow{k_0^*} \\ K_I^* \uparrow\downarrow \\ E^*\cdot Ca^{2+}\cdot I \xrightarrow{k_I^*} \end{array} \qquad \text{(A1)}$$

In the scheme above, the indicated inactivation rate constants are assumed to be different, depending on the binding state of the enzyme. If the binding reactions are fast and remain equilibrated throughout the process, the effective rate constant for inactivation is

$$k_{\text{inact}}{}^{\text{I}} = \frac{k_0^* + k_{\text{ND}}^*\frac{X_{\text{ND}}}{K_{\text{ND}}^*} + k_{\text{I}}^*\frac{X_{\text{I}}}{K_{\text{I}}^*}}{1 + \frac{X_{\text{ND}}}{K_{\text{ND}}^*} + \frac{X_{\text{I}}}{K_{\text{I}}^*}} = \frac{k_0^* + k_{\text{ND}}^*\frac{1}{K_{\text{ND}}^*} + X_{\text{I}}\left(\frac{k_{\text{I}}^*}{K_{\text{I}}^*} - \frac{k_{\text{ND}}^*}{K_{\text{ND}}^*}\right)}{1 + \frac{1}{K_{\text{ND}}^*} + X_{\text{L}}\left(\frac{1}{K_{\text{I}}^*} - \frac{1}{K_{\text{ND}}^*}\right)} \qquad \text{(A2)}$$

The last equality of eq A2 holds if $X_{ND} = 1 - X_I$, which is true if I is the only additive in the ND. When I is absent, the inactivation rate constant in eq A2 reduces to

$$k_{\text{inact}}{}^{0} = \frac{k_0^* + k_{\text{ND}}^*\frac{1}{K_{\text{ND}}^*}}{1 + \frac{1}{K_{\text{ND}}^*}} \qquad \text{(A3)}$$

To determine the dissociation constants with a Scrutton−Utter plot, one studies the ratio of half-times for inactivation in the presence (t_I*) and in the absence (t_{ND}*) of I as a function of $1/X_I$ in the following way:

$$\frac{1}{1 - \frac{t_{\text{ND}}^*}{t_{\text{I}}^*}} = \frac{1}{1 - \frac{k_{\text{inact}}{}^{\text{I}}}{k_{\text{inact}}{}^{0}}} = \left(1 - \frac{1}{X_{\text{I}}}\frac{1}{x\text{-intercept}}\right) y\text{-intercept} \qquad \text{(A4)}$$

This is a straight line, and by inserting eqs A2 and A3 into eq A4, one finds that the *x*-intercept is

$$x\text{-intercept} = -\frac{1}{K_{\text{I}}^*}\frac{1 - \frac{K_{\text{I}}^*}{K_{\text{ND}}^*}}{1 + \frac{1}{K_{\text{ND}}^*}} \approx -\frac{1}{K_{\text{I}}^*}\frac{1}{1 + \frac{1}{K_{\text{ND}}^*}} \qquad \text{(A5)}$$

The minus sign occurs because the line usually intercepts the *x*-axis on the negative side. Similarly, the *y*-intercept is found to be

$$y\text{-intercept} = \frac{1}{1 - \frac{(k_{\text{I}}^* - k_{\text{ND}}^*)\left(1 + \frac{1}{K_{\text{ND}}^*}\right)}{\left(k_0^* + k_{\text{ND}}^*\frac{1}{K_{\text{ND}}^*}\right)\left(1 - \frac{K_{\text{I}}^*}{K_{\text{ND}}^*}\right)}} \approx \frac{1}{1 - \frac{k_{\text{i}}^*\left(1 + \frac{1}{K_{\text{ND}}^*}\right)}{k_0^* + k_{\text{ND}}^*\frac{1}{K_{\text{ND}}^*}}} = \frac{1}{1 - \frac{k_{\text{I}}^*}{k_{\text{inact}}{}^{0}}} \qquad \text{(A6)}$$

The approximations in the second step of eqs A5 and A6 hold if I binds to enzyme much stronger than ND ($K_I^* \ll K_{ND}^*$) and if protection by I is not much more efficient than by ND ($k_I^*/k_{ND}^* \gg K_I^*/K_{ND}^*$).

From the *x*-intercept from eq A5, one can estimate the dissociation constant for I (K_I*), if only that of the ND (K_{ND}*) were known. Under some special circumstances, one can use the *y*-intercept from eq A6 to determine K_{ND}*. First, eq A3 can be solved for K_{ND}* to give

$$K_{\text{ND}}^* = \frac{1 - \frac{k_{\text{ND}}^*}{k_{\text{inact}}{}^{0}}}{\frac{k_0^*}{k_{\text{inact}}{}^{0}} - 1} \qquad \text{(A7)}$$

If all inhibitors bound at the active site provide the same protection, then $k_{ND}^* = k_I^*$ and eq A6 can be used in eq A7 to give

$$K_{\text{ND}}^* = \frac{1}{y\text{-intercept}}\frac{1}{\frac{k_0^*}{k_{\text{inact}}{}^{0}} - 1} = \frac{1}{y\text{-intercept}}\frac{1}{\frac{t_{\text{ND}}^*}{t_0^*} - 1} \qquad \text{(A8)}$$

Here, t_{ND}* is the inactivation time for the enzyme at the interface when it is at equilibrium between E*·Ca^{2+} and E*·Ca^{2+}·ND states, and t_0* is the inactivation time for the E*·Ca^{2+} state without any ligand at the active site. If k_I* and k_{ND}* are not exactly equal, eq A8 overestimates K_{ND}* by the amount ($k_{ND}^* - k_I^*$)/($k_0^* - k_{inact}{}^0$).

Effect of Calcium. Since calcium is required for the binding of ND and I to the active site of bvPLA2, the Scrutton−Utter analysis detailed above is carried out in the presence of saturating amounts of calcium. The effect of calcium on the rate of alkylation of bvPLA2 bound to D-LPC micelles is given by eq 5 of the main text, which is derived here. Since calcium has no effect on the rate of alkylation by PNBr in the absence of other ligands, it is assumed that the effect of calcium on protection is promotion of the binding of ligand in the active site of bvPLA2. Furthermore, it is assumed that D-LPC (or in general any neutral diluent) is present at sufficiently high concentrations so that essentially all enzyme is bound at the interface. Thus

$$\begin{array}{ccc} E^* & \xrightarrow{k_0^*} & \\ K^*_{Ca}(ND)\uparrow\downarrow & & \\ E^*\cdot Ca^{2+} & \xrightarrow{k_0^*} & \\ K^*_{ND}\uparrow\downarrow & & \\ E^*\cdot Ca^{2+}\cdot ND & \xrightarrow{k^*_{ND}} & \end{array}$$

In the absence of calcium, only the binding state E* is present, and the rate of inactivation is

$$k_{\text{inact}}{}^{0} = k_0{}^*$$

When calcium is present, the enzyme will be distributed over the three binding states in the diagram above. If these states are in rapid equilibrium on the time scale of inactivation, the effective rate constant of inactivation will be determined from the appropriate average over the binding states:

$$k_{\text{inact}}{}^{\text{Ca}} = \frac{k_0{}^*\left(1+\dfrac{[Ca^{2+}]}{K_{Ca}{}^*(ND)}\right) + k_{ND}{}^*\dfrac{[Ca^{2+}]}{K_{Ca}{}^*(ND)}\dfrac{1}{K_{ND}{}^*}}{1+\dfrac{[Ca^{2+}]}{K_{Ca}{}^*(ND)}\left(1+\dfrac{1}{K_{ND}{}^*}\right)}$$

Thus, after rearranging, one obtains eq 5 in the main text.

SUPPORTING INFORMATION AVAILABLE

Evaluation of the method of Burke et al. (1995) for demonstration of a neutral diluent (3 pages). Ordering information is given on any current masthead page.

REFERENCES

Annand, R. R., Kontoyianni, M., Penzotti, J. E., Dudler, T., Lybrand, T. P., & Gelb, M. H. (1996) *Biochemistry 35*, 4591−4601.

Bayburt, T., Yu, B. Z., Lin, H. K., Browning, J., Jain, M. K., & Gelb, M. H. (1993) *Biochemistry 32*, 573−582.

Berg, O. G., Yu, B.-Z., Rogers, J., & Jain, M. K. (1991) *Biochemistry 30*, 7283−7297.

Burke, J. R., Witmer, M. R., Tredup, J., Micanovic, R., Gregor, K. R., Lahiri, J., Tramposch, K. M., & Villafranca, J. J. (1995) *Biochemistry 34*, 15165−15174.

Cajal, Y., Berg, O. G., & Jain, M. K. (1995) *Biochem. Biophys. Res. Commun. 210*, 746−752.

Cajal, Y., Rogers, J., Berg, O. G., & Jain, M. K. (1996) *Biochemistry 35*, 299−308.

Davidson, F. F., & Dennis, E. A. (1990) *J. Mol. Evol. 31*, 228−38.

Dennis, E. A. (1983) *Enzymes 16*, 307−353.

Dudler, T., Chen, W.-Q., Wang, S., Schneider, T., Annand, R. R., Dempcy, R. O., Crameri, R., Gmachl, M., Suter, M., & Gelb, M. H. (1992) *Biochim. Biophys. Acta 1165*, 201−210.

Dupureur, C. M., Yu, B.-Z., Jain, M. K., Noel, J. P., Deng, T., Li, Y., Byeon, I. L., & Tsai, M.-D. (1992) *Biochemistry 31*, 6402−6413.

Eibl, H., McIntyre, J. O., Fleer, E. A. M., & Fleischer, S. (1983) *Methods Enzymol. 98*, 623−632.

Ellens, H., Bentz, J., & Szoka, F. C. (1985) *Biochemistry 24*, 3099−3106.

Gelb, M. H., Jain, M. K., Hanel, A. M., & Berg, O. (1995) *Annu. Rev. Biochem. 64*, 653−688.

Ghomashchi, F., Yu, B.-Z., Berg, O., Jain, M. K., & Gelb, M. H. (1991a) *Biochemistry 30*, 7318−7329.

Ghomashchi, F., Yu, B.-Z., Jain, M. K., & Gelb, M. H. (1991b) *Biochemistry 30*, 9559−9569.

Gomez, F., Vandermeers, A., Vandermeers-Piret, M.-C., Herzog, R., Rathe, J., Stievenart, M., Winand, J., & Christophe, J. (1989) *Eur. J. Biochem. 186*, 23−33.

Hanel, A. M., Schuttel, S., & Gelb, M. H. (1993) *Biochemistry 32*, 5949−5958.

Hauser, H., Hinckley, C. C., Krebs, J., Levine, B. A., Phillips, M. C., & Williams, R. J. (1977) *Biochim. Biophys. Acta 468*, 364−377.

Heinrikson, R. L., Krueger, E. T., & Keim, P. S. (1977) *J. Biol. Chem. 252*, 4913−4921.

Hoekstra, D., Buist-Arkema, R., Klappe, K., & Reutelingsperger, C. P. M. (1993) *Biochemistry 32*, 14194−14202.

Jain, M. K., & Vaz, W. L. C. (1987) *Biochim. Biophys. Acta 905*, 1−8.

Jain, M. K., & Berg, O. (1989) *Biochim. Biophys. Acta 1002*, 127−156.

Jain, M. K., & Gelb, M. H. (1991) *Methods Enzymol. 197*, 112−125.

Jain, M. K., Rogers, J., Jahagirdar, D. V., Marecek, J. F., & Ramirez, F. (1986) *Biochim. Biophys. Acta 860*, 435−447.

Jain, M. K., Ranadive, G., Yu, B.-Z., & Verheij, H. M. (1991a) *Biochemistry 30*, 7330−7340.

Jain, M. K., Rogers, J., Berg, O., & Gelb, M. H. (1991b) *Biochemistry 30*, 7340−7348.

Jain, M. K., Tao, W., Rogers, J., Arenson, C., Eibl, H., & Yu, B.-Z. (1991c) *Biochemistry 30*, 10256−10268.

Jain, M. K., Yu, B.-Z., Rogers, J., Ranadive, G. N., & Berg, O. (1991d) *Biochemistry 30*, 7306−7317.

Jain, M. K., Yu, B. Z., & Berg, O. G. (1993) *Biochemistry 32*, 11319−11329.

Jain, M. K., Gelb, M. H., Rogers, J., & Berg, O. G. (1995) *Methods Enzymol. 249*, 567−614.

Kubelka, V., Altmann, F., Staudacher, E., Tretter, V., Marz, L., Hard, K., Kamerling, J. P., & Vliegenthart, J. F. (1993) *Eur. J. Biochem. 213*, 1193−1204.

Kuchler, K., Gmachl, M., Sippl, J., & Kreil, G. (1989) *Eur. J. Biochem. 184*, 249−254.

McIntyre, J. C., & Sleight, R. G. (1991) *Biochemistry 30*, 11819−11827.

Ramirez, F., & Jain, M. K. (1991) *Proteins 9*, 229−239.

Scott, D. L., & Sigler, P. B. (1994) *Adv. Protein Chem. 45*, 53−88.

Scott, D. L., Otwinowski, Z., Gelb, M. H., & Sigler, P. B. (1990) *Science 250*, 1563−1566.

Scott, D. L., Mandel, A. M., Sigler, P. B., & Honig, B. (1994) *Biophys. J. 67*, 493−504.

Shipolini, R. A., Callewaert, G. L., Cottrell, R. C., & Vernon, C. A. (1974) *Eur. J. Biochem. 48*, 465−476.

Sosa, B. P., Alagon, A. C., Martin, B. M., & Possani, L. D. (1986) *Biochemistry 25*, 2927−2933.

van den Bergh, C. J., Slotboom, A. J., Verheij, H. M., & De Haas, G. H. (1989) *J. Cell. Biochem. 39*, 379−390.

Verheij, H. M., Slotboom, A. J., & De Haas, G. H. (1981) *Rev. Physiol. Biochem. Pharmacol. 91*, 91−203.

Waite, M. (1987) *The Phospholipases*, Plenum, New York.

Yu, B.-Z., Berg, O. G., & Jain, M. K. (1993) *Biochemistry 32*, 6485−6492.

Yuan, W., Quinn, D. M., Sigler, P. B., & Gelb, M. H. (1990) *Biochemistry 29*, 6082−6094.

BI961541X